

## **Isoreticular Chemistry of Scandium Analogues of the Multicomponent Metal-Organic Framework MIL-142**

Ram R. R. Prasad,<sup>\*a,b</sup> Charlotte Pleass,<sup>a</sup> Amber L. Rigg,<sup>a</sup> David B. Cordes,<sup>a</sup> Magdalena M. Lozinska,<sup>a</sup> Veselina M. Georgieva,<sup>a</sup> Frank Hoffmann,<sup>c</sup> Alexandra M. Z. Slawin,<sup>a</sup> and Paul A. Wright <sup>\*a</sup>

<sup>a</sup> EaStCHEM School of Chemistry, University of St Andrews, Purdie Building, North Haugh, St Andrews, KY16 9ST, UK.

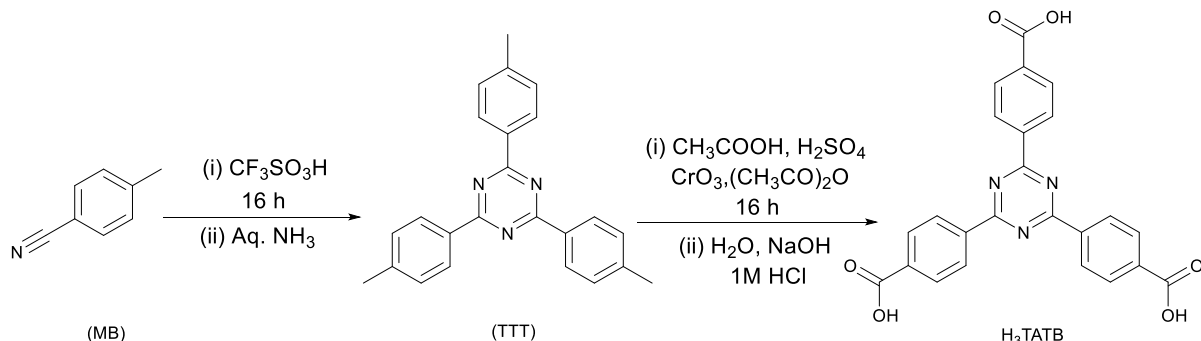
<sup>b</sup> Current Address: Department of Chemistry, Dainton Building, The University of Sheffield, Brook Hill, Sheffield, S3 7HF.

<sup>c</sup> Institute of Inorganic and Applied Chemistry, Department of Chemistry, University of Hamburg, Martin-Luther-King-Platz 6, 20146 Hamburg, Germany.

E-mail: r.ramprasad@sheffield.ac.uk, paw2@st-andrews.ac.uk

## Synthesis of 4,4',4''-(1,3,5-triazine-2,4,6-triyl)tribenzoic acid (TATB)

TATB was synthesised in two steps combining two synthesis procedures in the literature.<sup>1,2</sup>



**Scheme SS1:** Synthesis of H<sub>3</sub>TATB.

**Synthesis of 2,4,6-tri-p-tolyl-1,3,5-triazine (TTT):** Modification of the reported procedure.<sup>1</sup> To 14.63 mL (166 mmol) of trifluoromethanesulfonic acid in a round-bottom flask, 7 g (60 mmol) of 4-methylbenzonitrile was added slowly in portions over a period of 2 h. After stirring at room temperature overnight, the resulting orange mixture was poured into ice-water and neutralized with aq. ammonia solution and stirred for 2 h. The white precipitate obtained was filtered and washed with water: acetone (1:1) multiple times and dried overnight at 80 °C. On recrystallisation from hot toluene, white needle shaped crystals were obtained. Yield = 14.35 g (68%). <sup>1</sup>H NMR (400 MHz, CDCl<sub>3</sub>) δ (ppm): 8.68 (6H, d, *J* = 8.2 Hz), 7.36 (6H, d, *J* = 8.19 Hz), 2.51 (9H, s). Data in accordance with literature.<sup>1</sup>

**Synthesis of 4,4',4''-(1,3,5-triazine-2,4,6-triyl)tribenzoic acid (TATB):** To a 250 mL round-bottom flask equipped with a magnetic stirrer, 2.78 g (7.9 mmol) of 2,4,6-tri-p-tolyl-1,3,5-triazine was added, followed by 70 mL acetic acid. 4.4 mL H<sub>2</sub>SO<sub>4</sub> was added slowly until the solution became clear. Then, keeping the flask in an ice-cold water bath, 7.2 g (72 mmol) of Cr(VI)O<sub>3</sub> dissolved in 4.8 mL of acetic anhydride was added dropwise. Care was taken with handling of pyrophoric CrO<sub>3</sub>. After complete addition and stirring for 15 minutes, the water bath was removed, and the resulting dark brown slurry was stirred at room temperature overnight. The mixture was then poured into 300 mL water and stirred for 2 h, filtered and washed multiple times with copious amounts of water. The resulting solid was then dissolved in 200 mL of NaOH solution (2 M) and filtered to remove unreacted starting materials. The filtrate was acidified with HCl (1 M) to obtain 4,4',4''-(1,3,5-triazine-2,4,6-triyl)tribenzoic acid as a white precipitate, which was washed with water several times and dried at 80 °C.

overnight. Yield = 2.8 g (80%).  $^1\text{H}$  NMR (400 MHz,  $\text{CDCl}_3$ )  $\delta$  (ppm): 8.88 (6H, d,  $J$  = 8.24 Hz), 8.21 (6H, d,  $J$  = 8.21 Hz). Data in accordance with literature.<sup>2</sup>

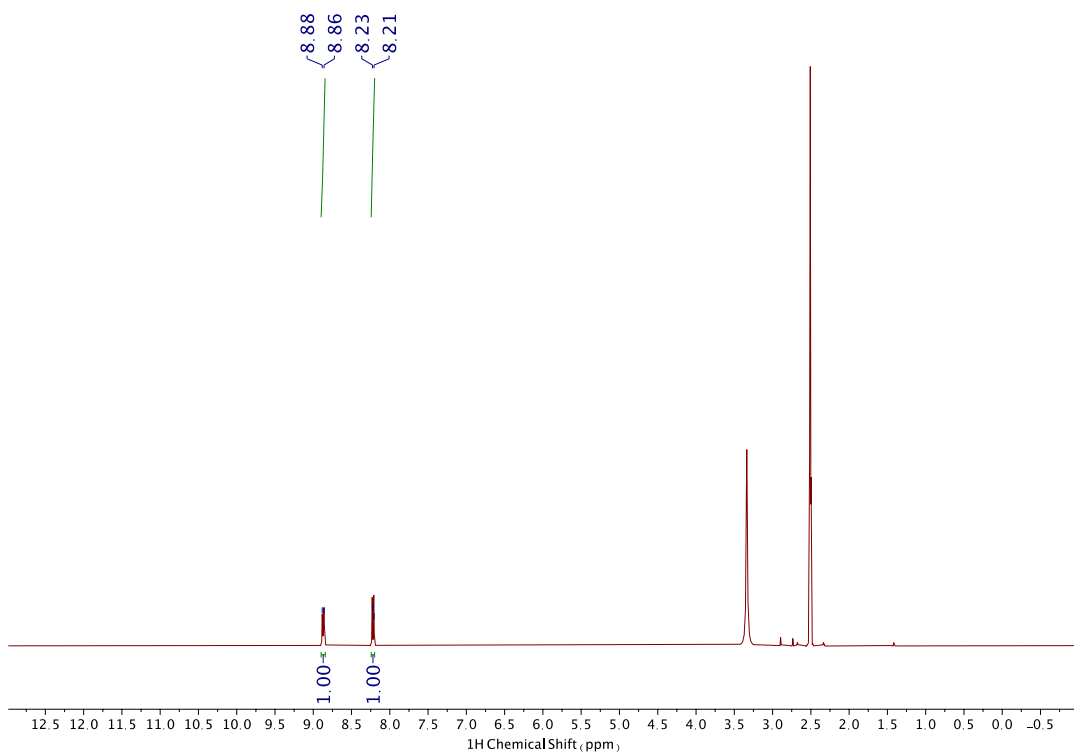


**Figure S1:**  $^1\text{H}$  NMR of  $\text{H}_3\text{TATB}$ .

## Synthesis of 4,4',4''-(pyridine-2,4,6-triyl)tribenzoic acid (H<sub>3</sub>PTB)

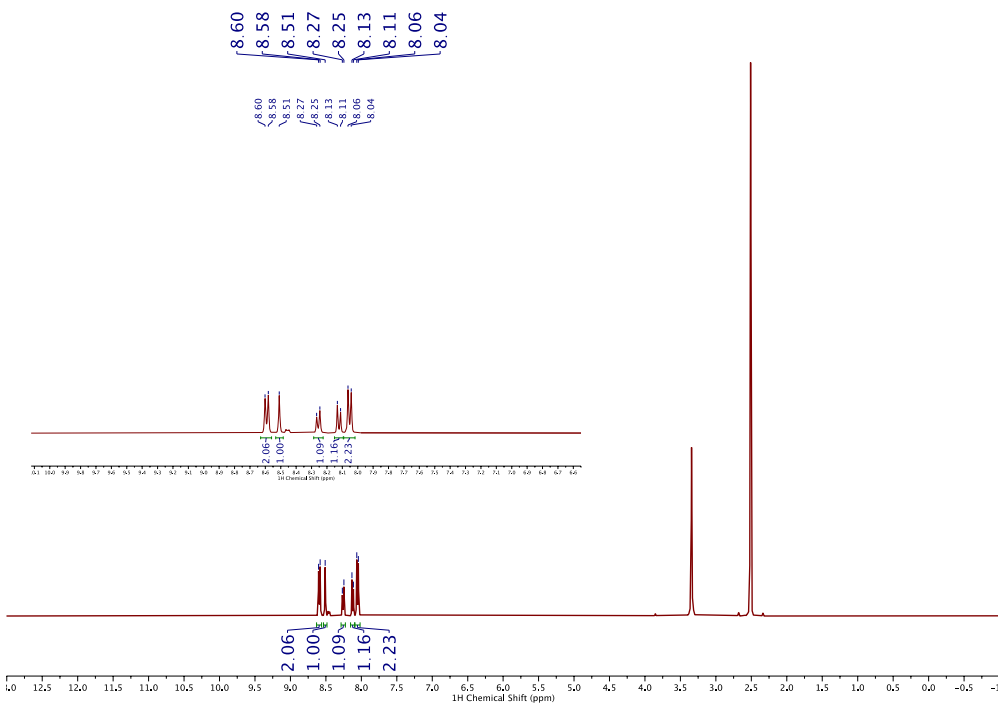


**Figure S2:**  $^1\text{H}$  NMR of BCPB.

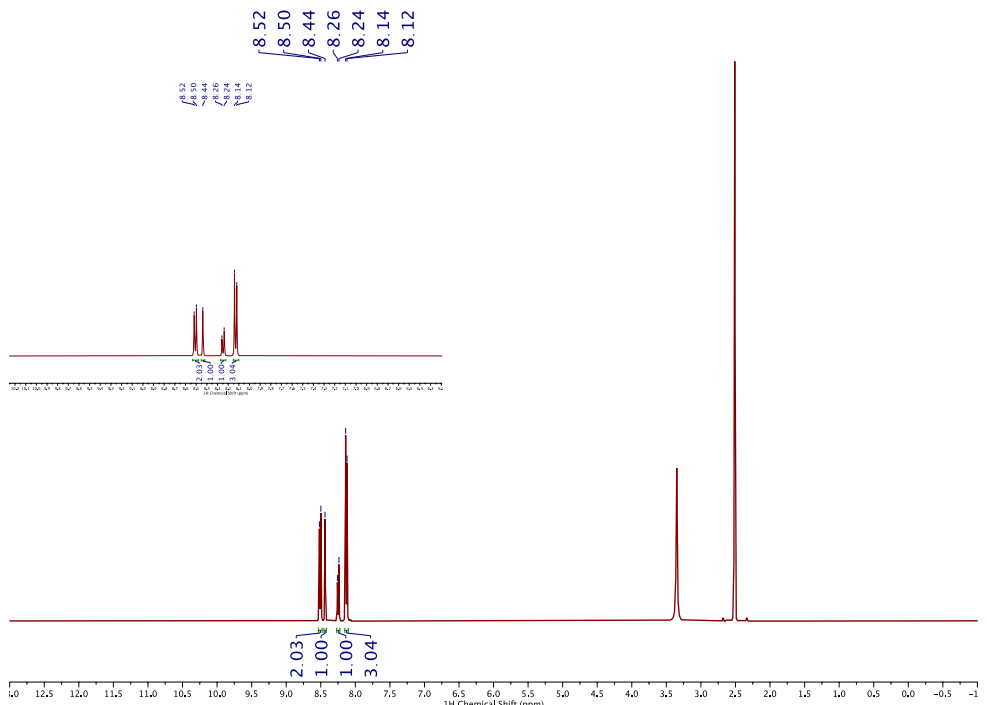


**Figure S3:**  $^1\text{H}$  NMR of  $\text{H}_3\text{PTB}$ .

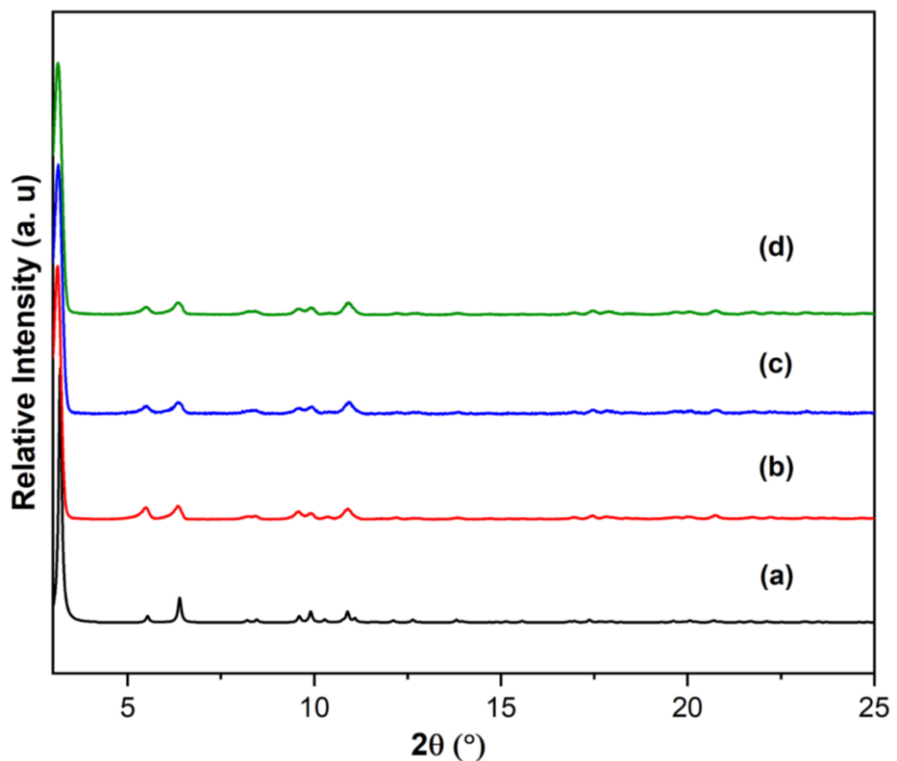


**Figure S4:** Simulated PXRD pattern of (a) InPF-110 with PXRD patterns of (b) Sc-BTB synthesised under optimised conditions, (c) Sc-BTB-BDC synthesised using 0.9 mmol  $\text{ScCl}_3$ , 0.5 mmol BTB, 0.5 mmol BDC and (d) Sc-BTB-BDC synthesised using 0.75 mmol  $\text{ScCl}_3$ , 0.5 mmol BTB, 0.5 mmol BDC.

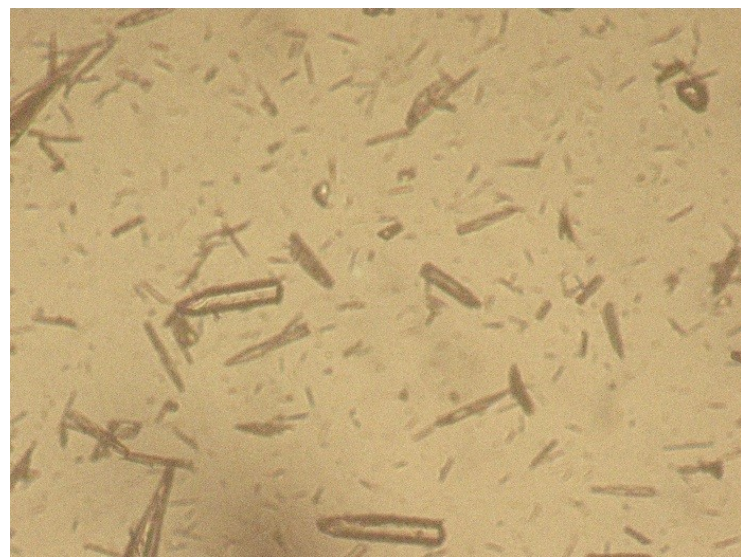


**Figure S5:** Single crystals of Sc-BTB.

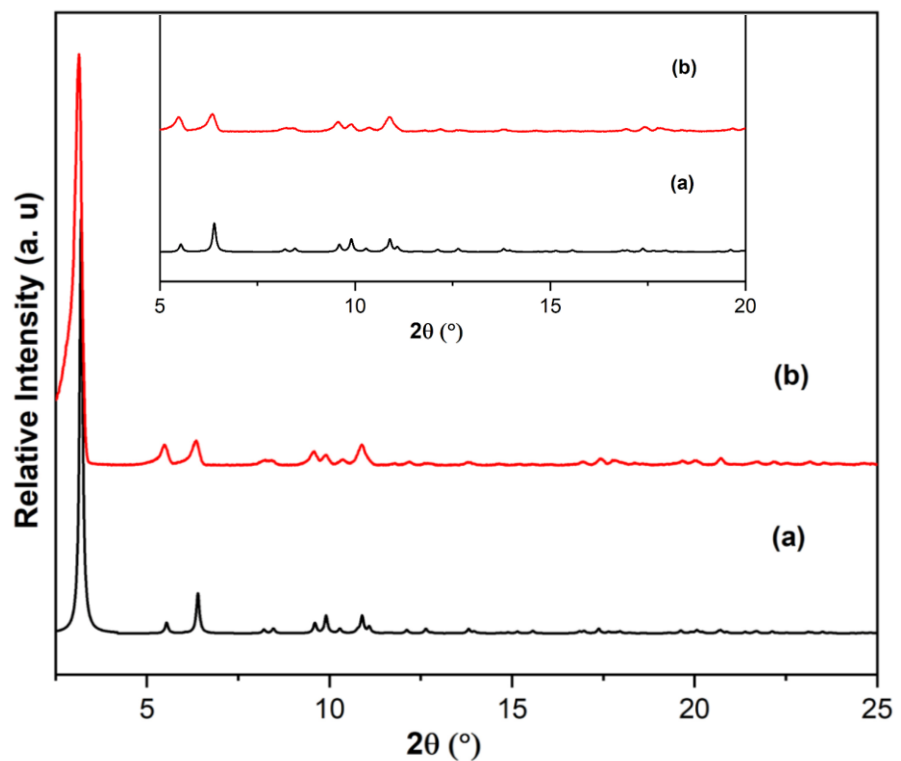


**Figure S6:** Simulated PXRD pattern of (a) InPF-110 with PXRD pattern of (b) Sc-BTB. The inset shows expanded view of the patterns.

**Table ST1:** Crystallographic Table for Sc-BTB

Sc-BTB	
Formula	C <sub>58</sub> H <sub>38</sub> NO <sub>16</sub> Sc <sub>3</sub>
Formula weight (g mol <sup>-1</sup> )	1139.80
Temperature (K)	173(2)
Crystal System	Hexagonal
Space group	P <sup>6</sup> 2c
a (Å)	31.8080(16)
c (Å)	16.9754 (8)
V (Å)	14873.8(13)
Z	6
ρ(calcd) (g cm <sup>-3</sup> )	0.763
μ (mm <sup>-1</sup> )	2.042
F(000)	3504
Reflections collected	150898
Unique reflections (R <sub>int</sub> )	9344 (0.1139)
GoF	1.037
Final R <sub>1</sub> values [ <i>I</i> >2σ( <i>I</i> )]	0.0405
Final wR <sub>2</sub> values (all data)	0.1124

**Table ST2:** Different Sc-O bond lengths in Sc-BTB framework

Bond	Bond lengths (Å)
Sc-O (carboxylates)	2.123, 2.086, 2.089, 2.100, 2.098, 2.149
Sc- $\mu_3$ O (DMF coordinated)	1.980
Sc- $\mu_3$ O (formate bridging)	2.035
Sc-O (formate)	2.132
Sc-O (DMF)	2.210

**Table ST3:** Synthesis conditions for Sc-BTB, Sc-PTB and PCN-333(Sc)

MOF	Metal Source	Linker	DMF (mL)	HNO <sub>3</sub> (mL)	Temp (°C)	Time (h)	Phase purity
Sc-BTB	Sc(NO <sub>3</sub> ) <sub>3</sub> .xH <sub>2</sub> O	BTB	2.5	0.8	150	4	Crystalline
Sc-PTB	Sc(NO <sub>3</sub> ) <sub>3</sub> .xH <sub>2</sub> O	PTB	2.5	0.8	150	4	Crystalline
PCN-333(Sc)	Aq. ScCl <sub>3</sub>	TATB	10	-	150	20	Less crystalline

Note: Sc(NO<sub>3</sub>)<sub>3</sub>.xH<sub>2</sub>O prior to usage was dried at 378 K overnight. For Sc-BTB and Sc-PTB, 0.33 mmol Sc(NO<sub>3</sub>)<sub>3</sub>.xH<sub>2</sub>O and 0.15 mmol BTB/PTB was used. For PCN-333(Sc), 0.45 mmol aq. ScCl<sub>3</sub> and 0.90 mmol TATB was employed. PCN-333(Sc) was synthesised adapting the procedure reported by Zhou and co-workers.<sup>2</sup> 397.3 mg TATB (0.90 mmol) was weighed out into a Teflon liner (~ 30 mL total volume) containing a magnetic stirrer. After the addition of 10 mL DMF, 0.3 mL (1.5 M) of aqueous ScCl<sub>3</sub> solution was added and stirred at room temperature for 1 h. The Teflon liner was then transferred into a stainless-steel autoclave and heated at 423 K for 20 h. After cooling to room temperature and the precipitate obtained was collected by vacuum filtration and washed multiples times with DMF and methanol before being dried.

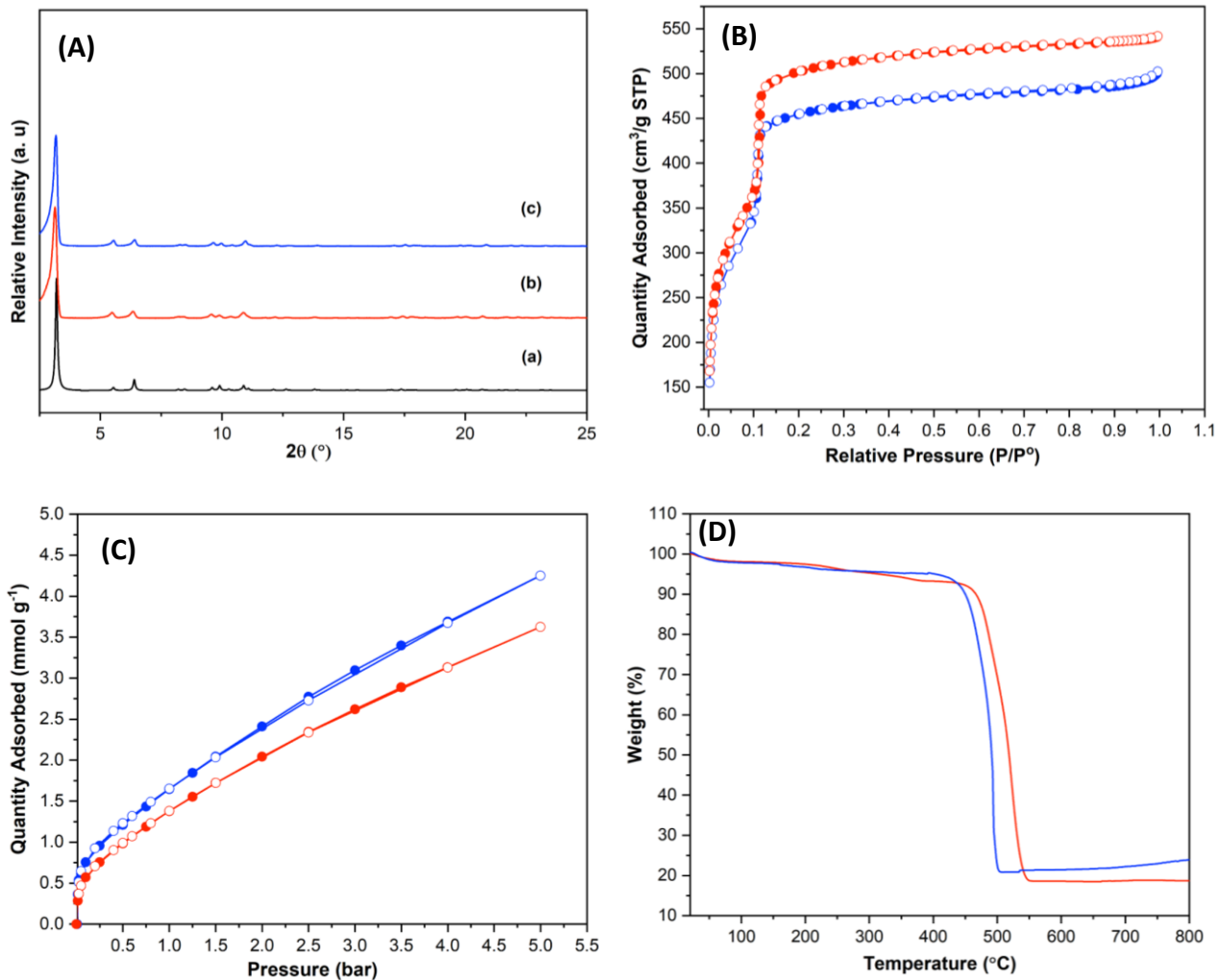


**Figure S7:** (A) PXRD, (B)  $N_2$  adsorption isotherms, (C)  $\text{CO}_2$  adsorption isotherms and (D) TGA of Sc-BTB (red) and Sc-PTB (blue). Note: In figure (A), simulated PXRD pattern for Sc-BTB (a, black) from SCXRD structure is given along with PXRD patterns of Sc-BTB and Sc-PTB for comparison.

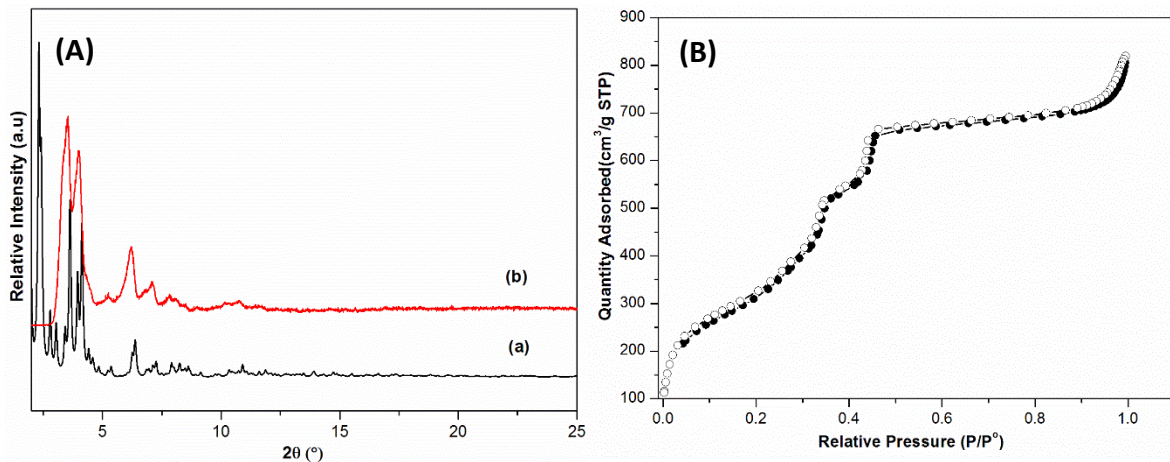


**Figure S8:** (A) Simulated PXRD patterns of PCN-333(Sc) (a, black) compared with the PXRD pattern of as-synthesised PCN-333(Sc) (b, red) and (B)  $N_2$  adsorption-desorption isotherms at  $-196^{\circ}\text{C}$  for PCN-333(Sc) after activation at  $150^{\circ}\text{C}$  for 16 h.

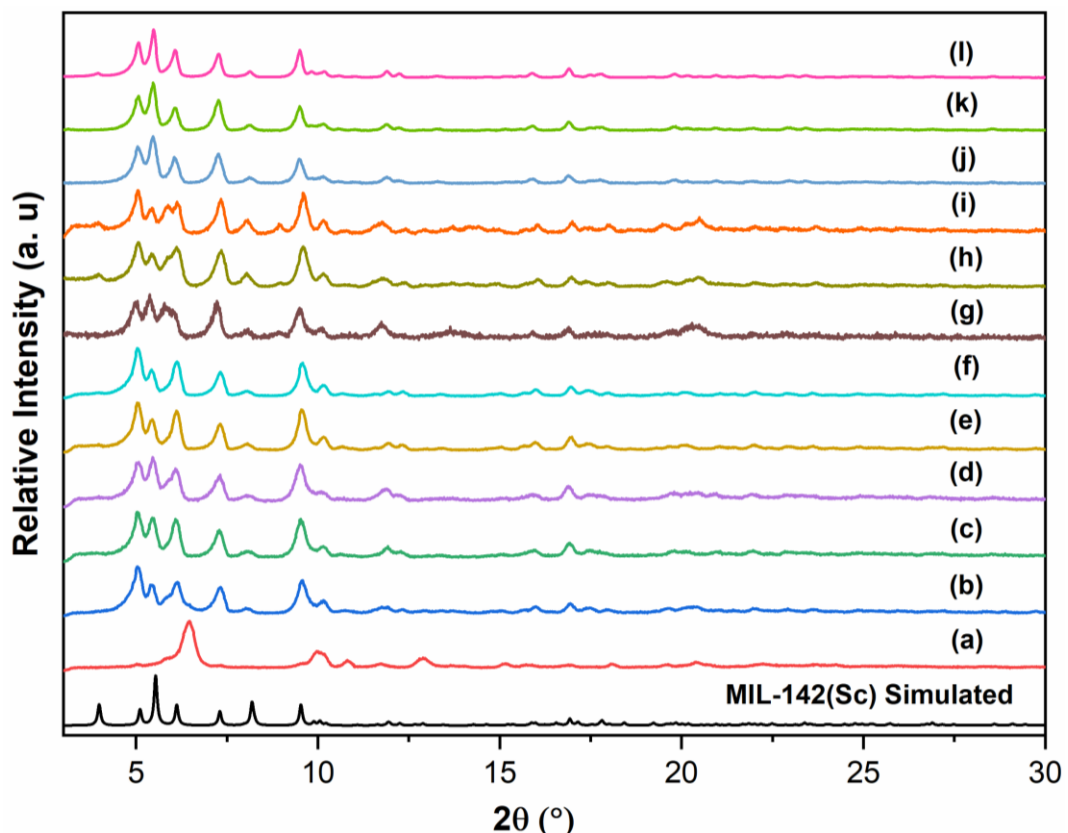


**Figure S9:** PXRD of synthesis optimization for MIL-142(Sc)-TATB. Detailed aq. ScCl<sub>3</sub>:BDC:TATB ratios is given in Table 2. Solvent- DMF (3 mL); temperature, 423 K; time, 30 h.

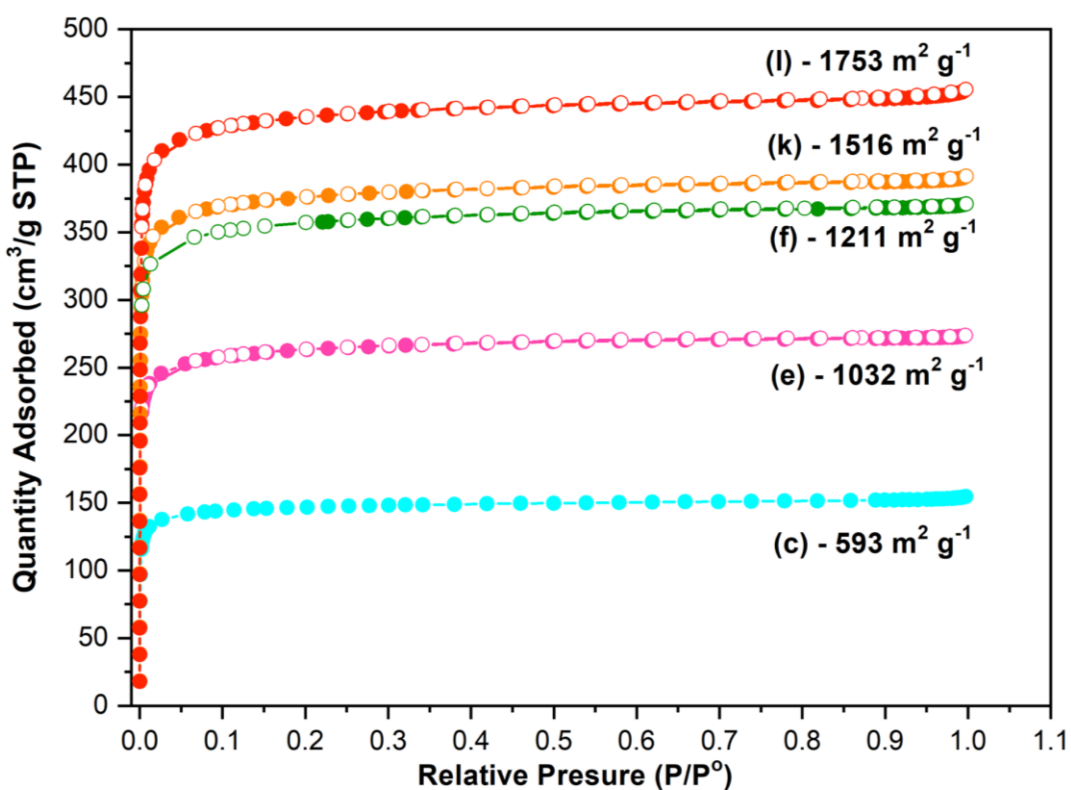


**Figure S10:** N<sub>2</sub> adsorption-desorption isotherms at 77 K for selected samples of MIL-142(Sc)-TATB from figure S3 after activation at 423 K for 16 h.

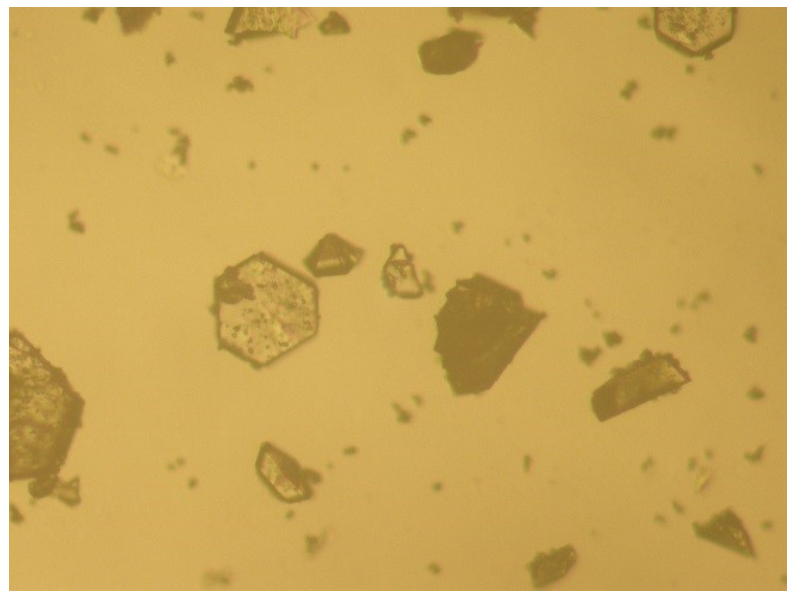


**Figure S11:** Single crystals of MIL-142(Sc)-TATB.

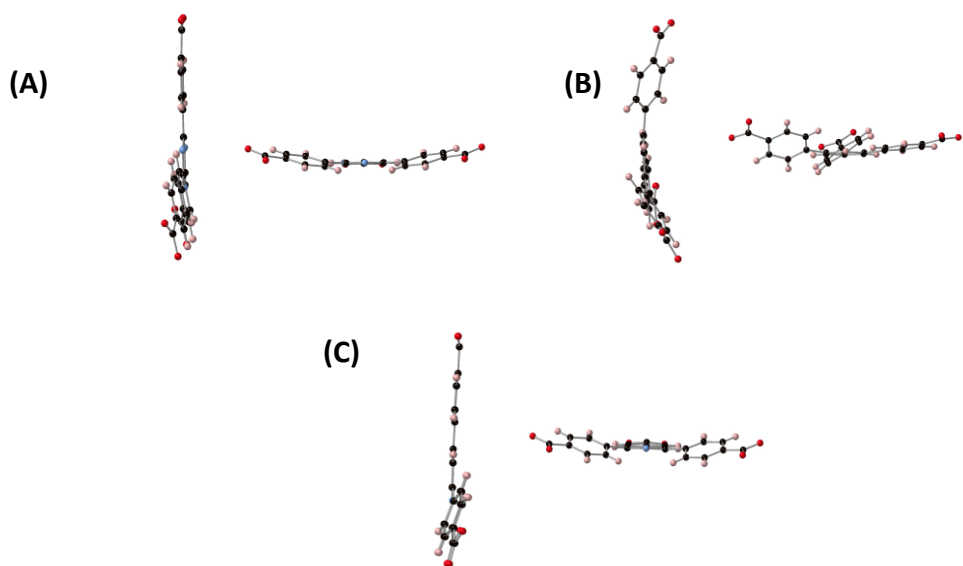


**Figure S12:** Geometries of different tricarboxylic acid linkers: (A) TATB, (B) BTB, and (C) PTB.

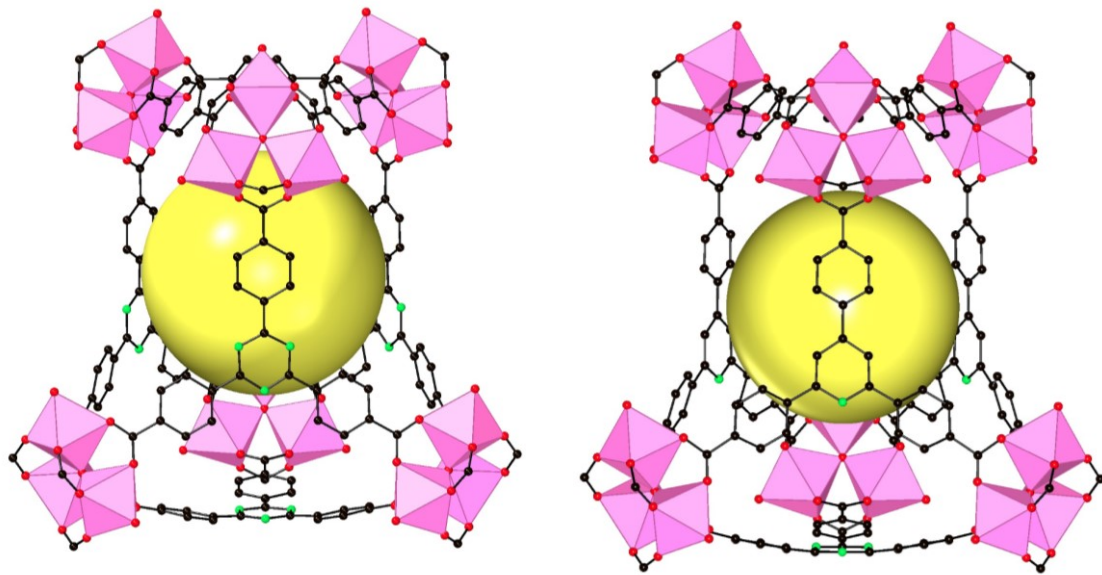


**Figure S13:** The superoctahedral cages of (left) MIL-142(Sc)-TATB and (right) MIL-142(Sc)-PTB.C/N atoms of the base PTB linker in MIL-142(Sc)-PTB is disordered.

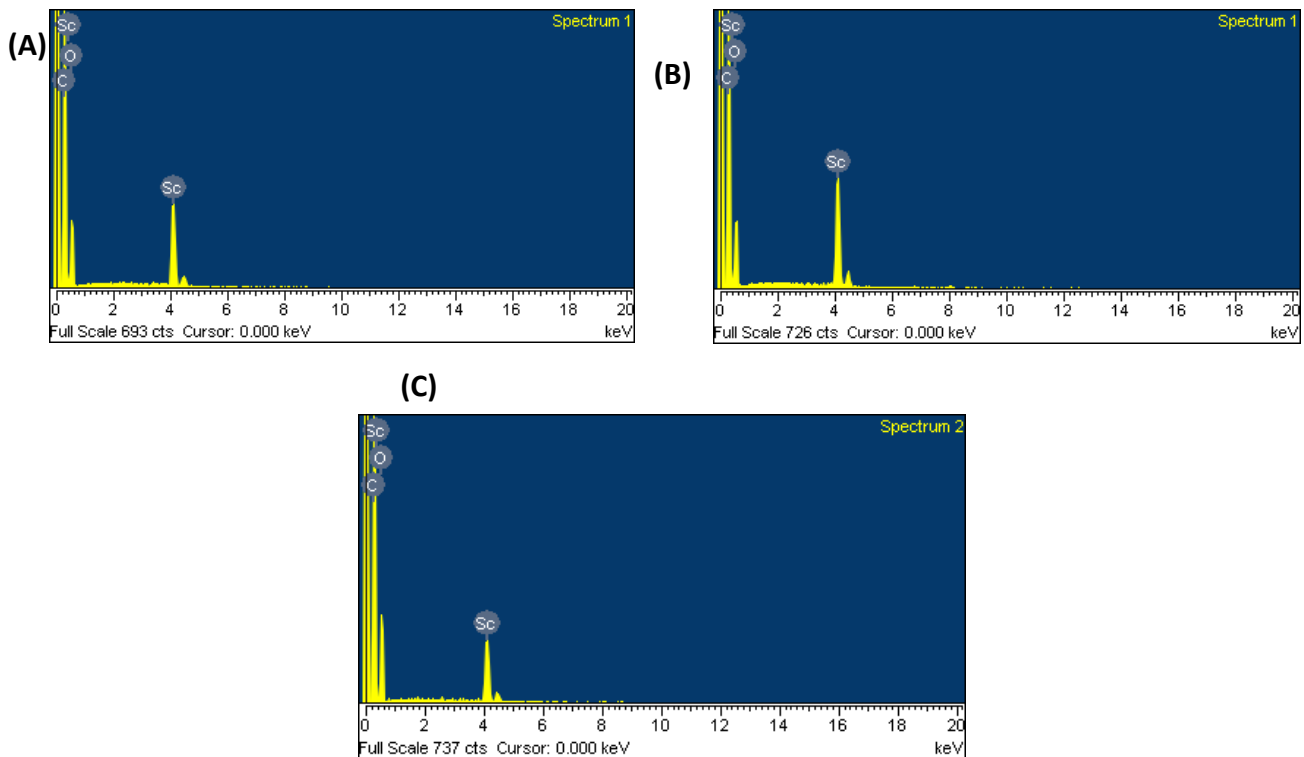


**Figure S14:** EDX spectra of (a) MIL-142(Sc)-TATB, (b) MIL-142(Sc)-TATB-NH<sub>2</sub> and (c) MIL-142(Sc)-TATB-NO<sub>2</sub>.

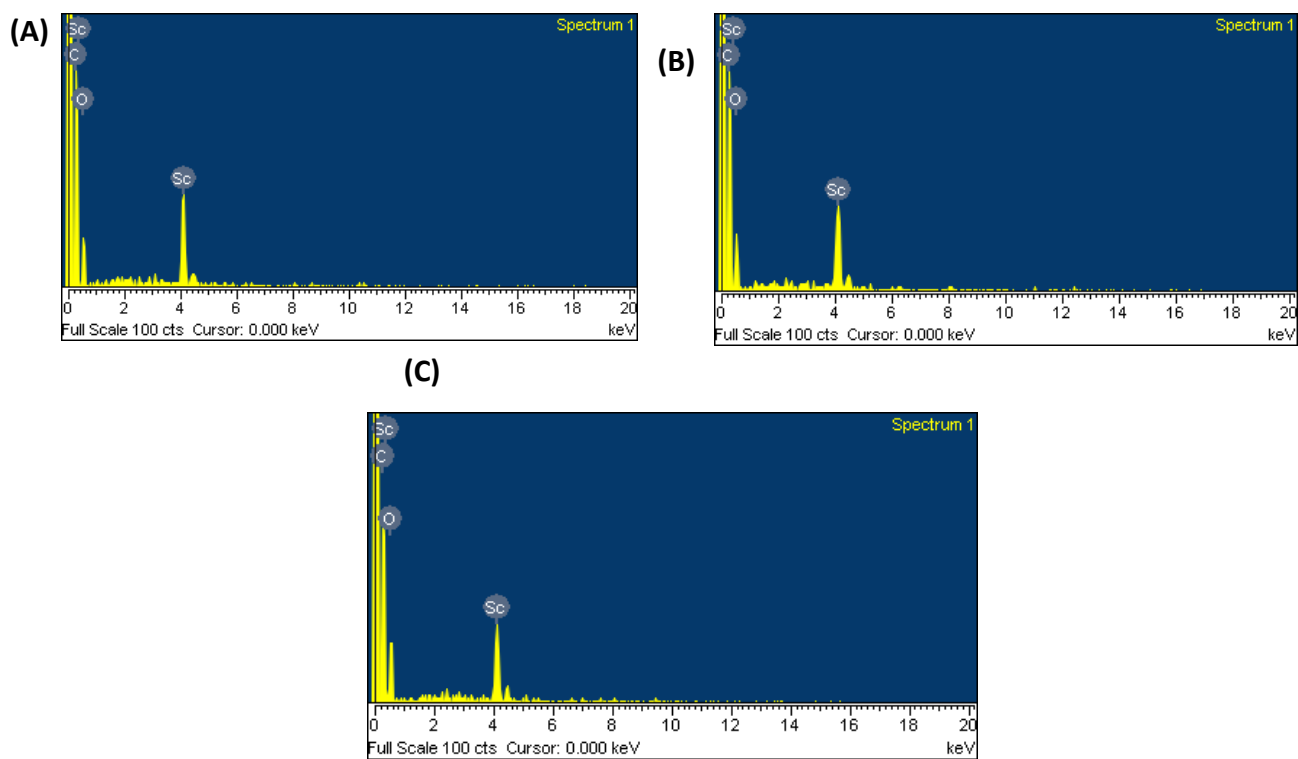


**Figure S15:** EDX spectra of (a) MIL-142(Sc)-PTB, (b) MIL-142(Sc)-PTB-NH<sub>2</sub> and (c) MIL-142(Sc)-PTB-NO<sub>2</sub>.

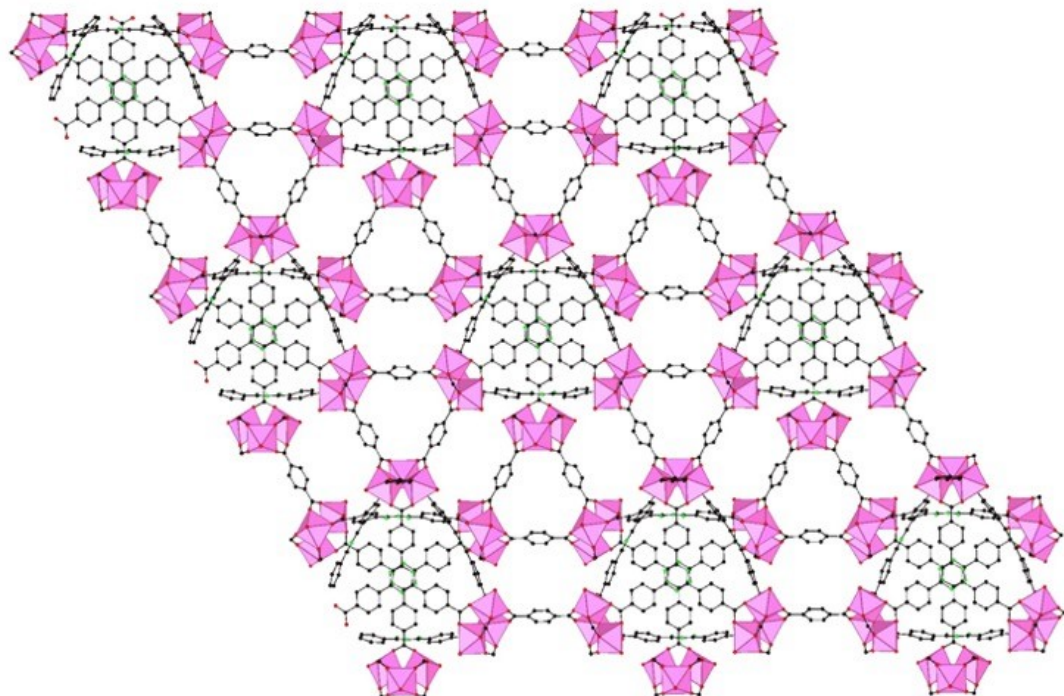


**Figure S16:** TATB bridges between the top triangles of the nearby superoctahedra of MIL-142(Sc)-TATB.

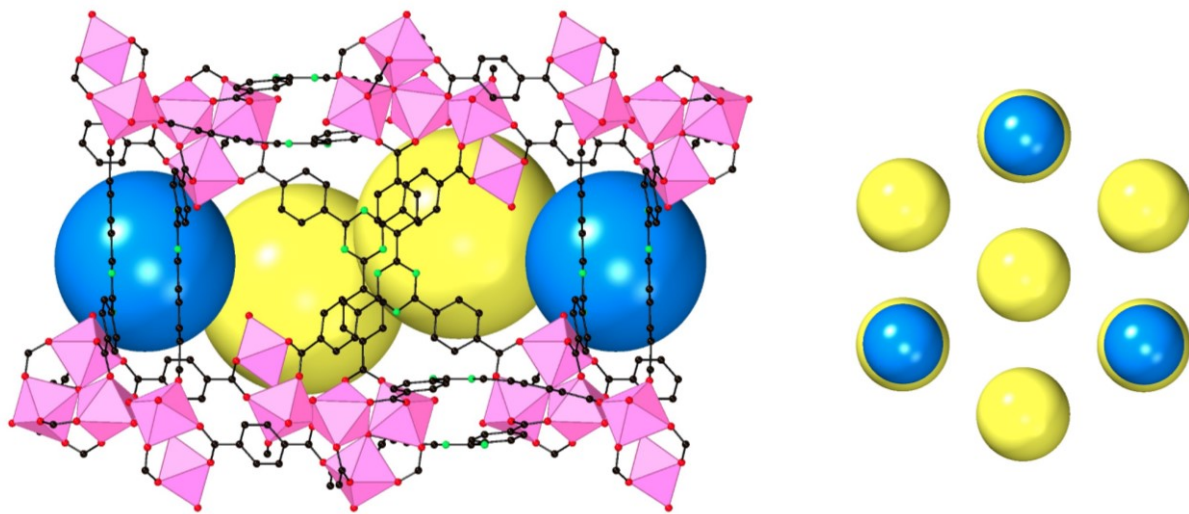


**Figure S17:** Pore connectivity of MIL-142(Sc)-TATB in the *ab* plane.

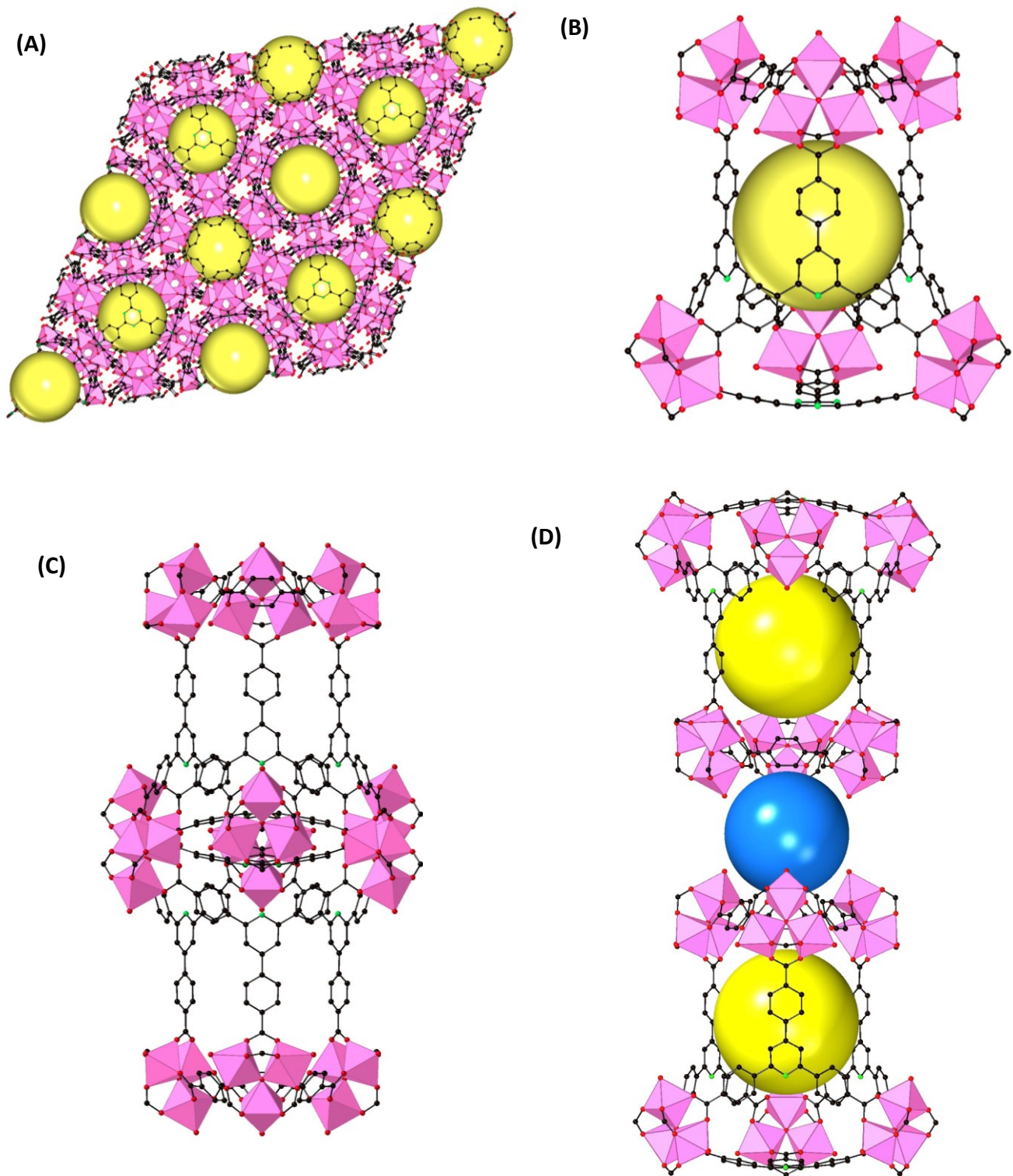
**Table ST4:** Different Sc-O bond lengths in MIL-142(Sc)-TATB framework

Bond	Bond lengths (Å)
Sc-O (carboxylates)	2.085(18) to 2.1050(17)
Sc- $\mu_3$ O	2.002(2), 2.0253(11)
Sc-OH, Ow	2.162(2), 2.185(2)

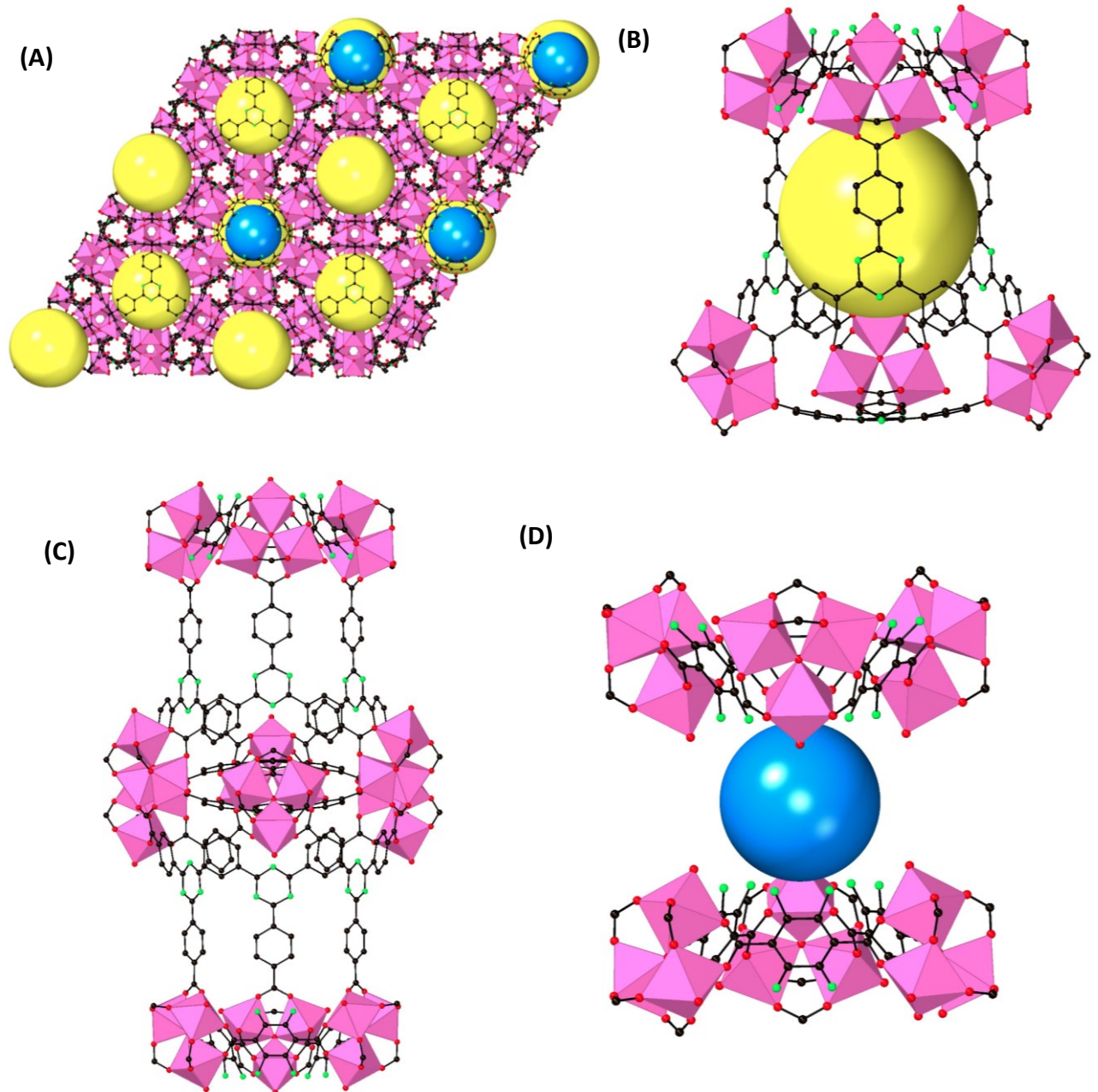
**Table ST5:** Different Sc-O bond lengths in MIL-126(Sc) and MIL-88(Sc)

Bond	Bond lengths (Å)
Sc-O (carboxylates)	2.082, 2.102, 2.118
Sc- $\mu_3$ O	2.012, 2.022
Sc-OH/X/Ow	2.093

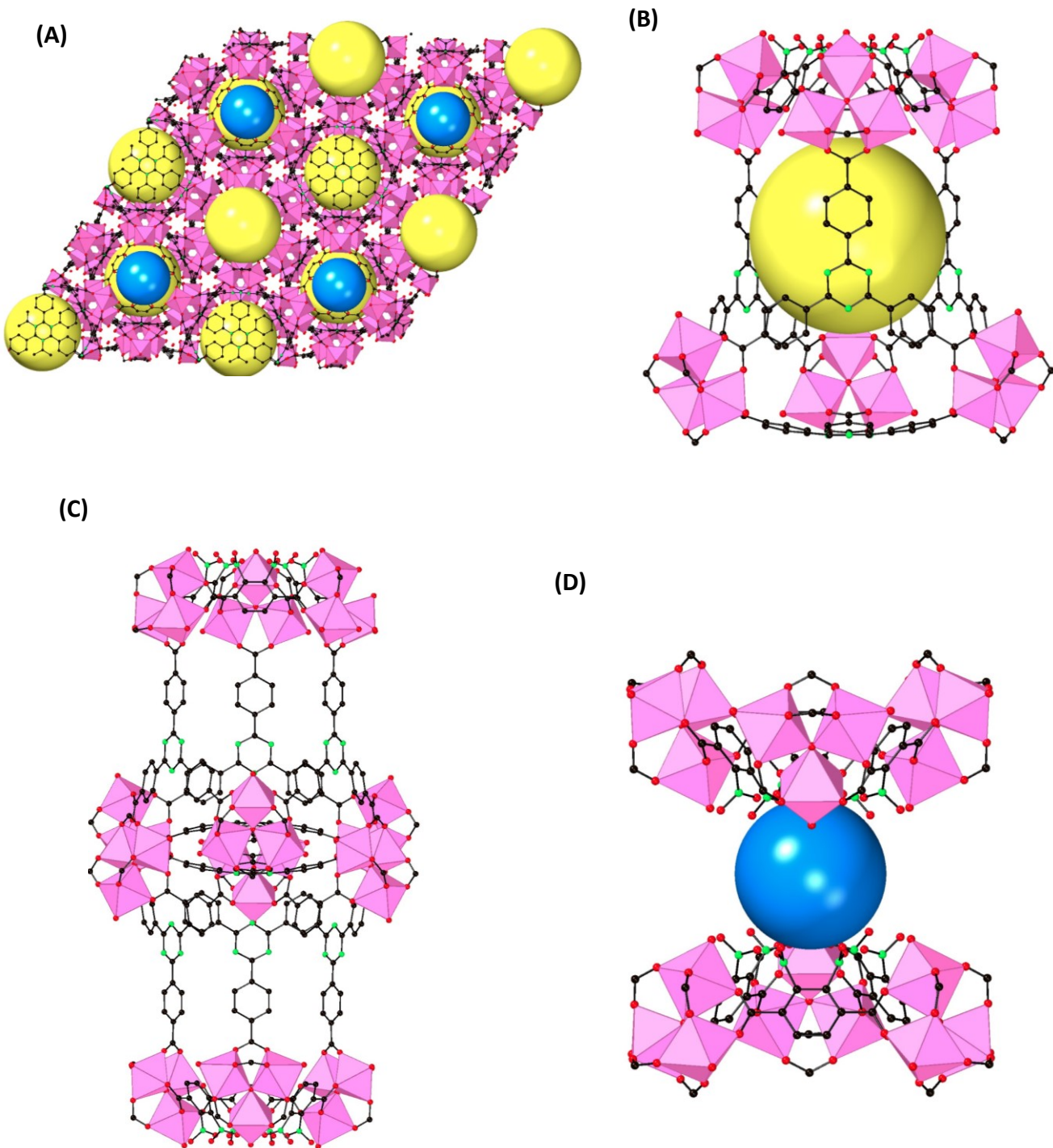
Note: X stands for charge balancing OH<sup>-</sup> or Cl<sup>-</sup>.



**Figure S18:** Crystal structure of MIL-142(Sc)-PTB. (a) The overall two-fold interpenetrated structure of MIL-142(Sc)-PTB, (b) the superoctahedra of MIL-142(Sc)-PTB in which the  $\text{Sc}_3$  trimers are connected by BDC and PTB linkers, (c) the interpenetrated superoctahedra and (d) the superoctahedra with small cage between them. Cages are represented by yellow and blue spheres. Colour code: Sc, pink; C, black; N, green; O, red. C/N atoms of the base PTB linker in MIL-142(Sc)-PTB is disordered.

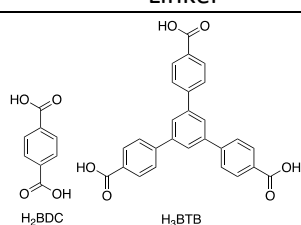
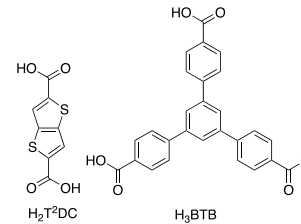
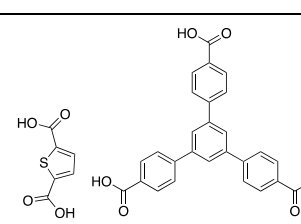
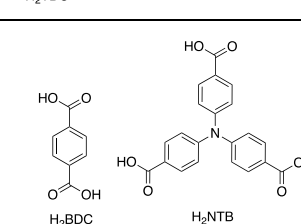
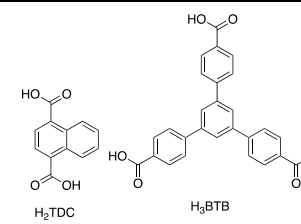
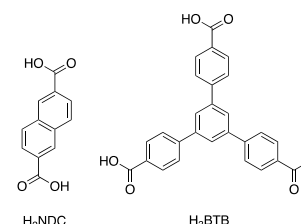


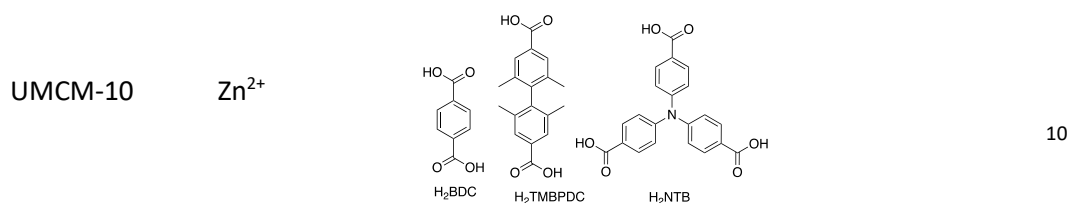
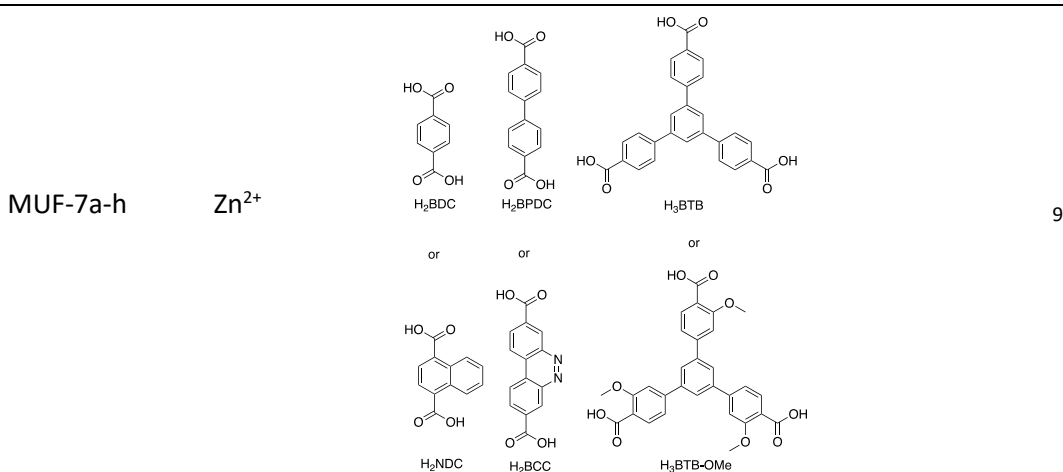
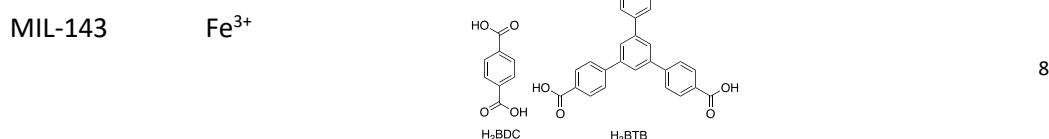
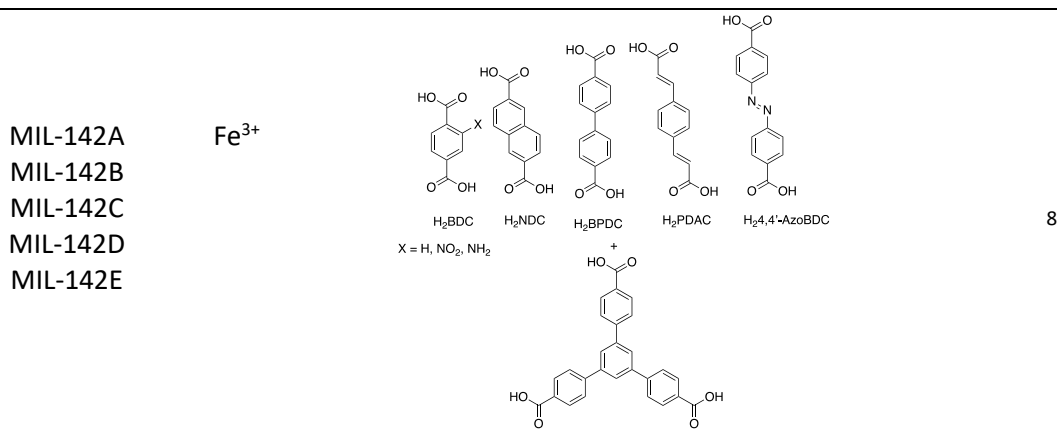
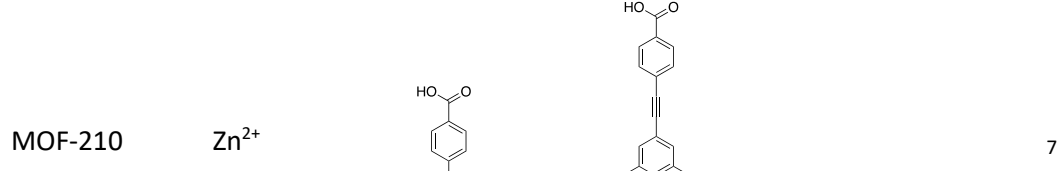
**Figure S19:** Crystal structure of MIL-142(Sc)-TATB-NH<sub>2</sub>. (a) The overall two-fold interpenetrated structure of MIL-142(Sc)-TATB-NH<sub>2</sub>, (b) the superoctahedra of MIL-142(Sc)-TATB-NH<sub>2</sub> in which the Sc<sub>3</sub> trimers are connected by NH<sub>2</sub>-BDC and TATB linkers, (c) the interpenetrated superoctahedra and (d) the superoctahedra with small cage between them. Cages are represented by yellow and blue spheres. Colour code: Sc, pink; C, black; N, green; O, red.



**Figure S20:** Crystal structure of MIL-142(Sc)-TATB-NO<sub>2</sub>. (a) The overall two-fold interpenetrated structure of MIL-142(Sc)-TATB-NO<sub>2</sub>, (b) the superoctahedra of MIL-142(Sc)-TATB-NO<sub>2</sub> in which the Sc<sub>3</sub> trimers are connected by NO<sub>2</sub>-BDC and TATB linkers, (c) the interpenetrated superoctahedra and (d) the superoctahedra with small cage between them. Cages are represented by yellow and blue spheres. Colour code: Sc, pink; C, black; N, green; O, red.

**Table ST6:** Multicomponent MOFs reported till now with di and tricarboxylate linkers

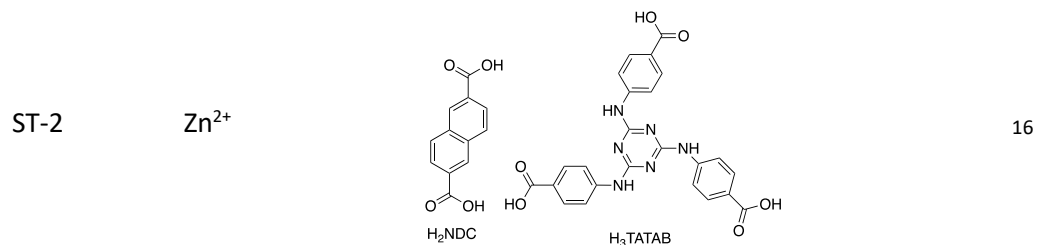
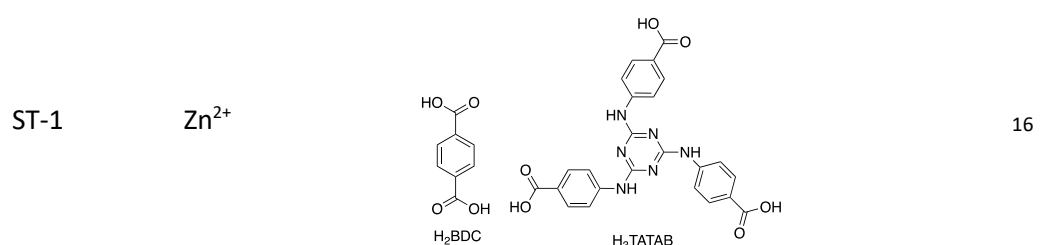
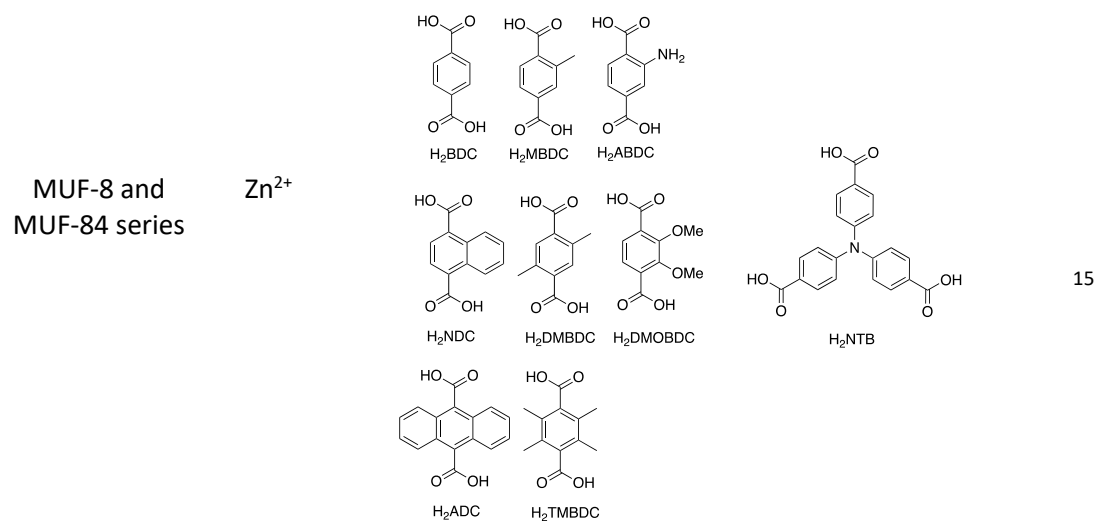
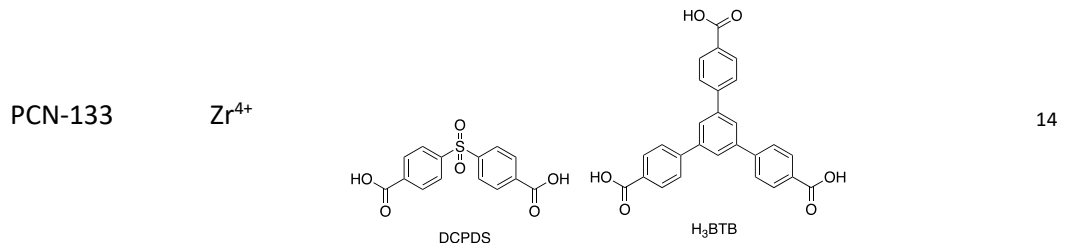
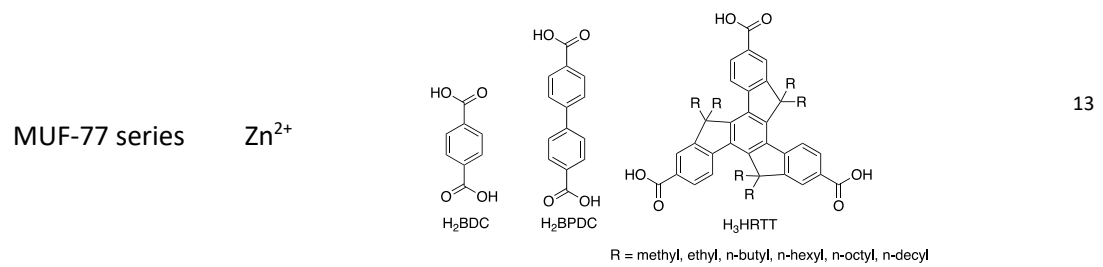
MOF	Metal	Linker	Ref
UMCM-1	Zn <sup>2+</sup>	 H <sub>2</sub> BDC      H <sub>3</sub> BTB	3
UMCM-2	Zn <sup>2+</sup>	 H <sub>2</sub> T'DC      H <sub>3</sub> BTB	4
UMCM-3	Zn <sup>2+</sup>	 H <sub>2</sub> TDC      H <sub>3</sub> BTB	5
UMCM-4	Zn <sup>2+</sup>	 H <sub>2</sub> BDC      H <sub>2</sub> NTB	5
UMCM-5	Zn <sup>2+</sup>	 H <sub>2</sub> TDC      H <sub>3</sub> BTB	5
DUT-6 MOF-205	Zn <sup>2+</sup>	 H <sub>2</sub> NDC      H <sub>3</sub> BTB	6, 7

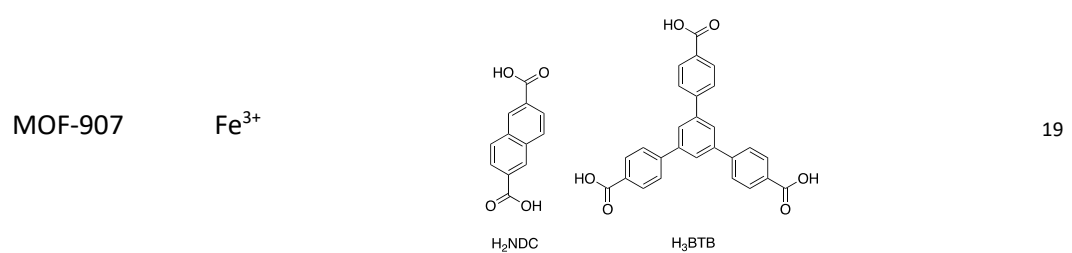
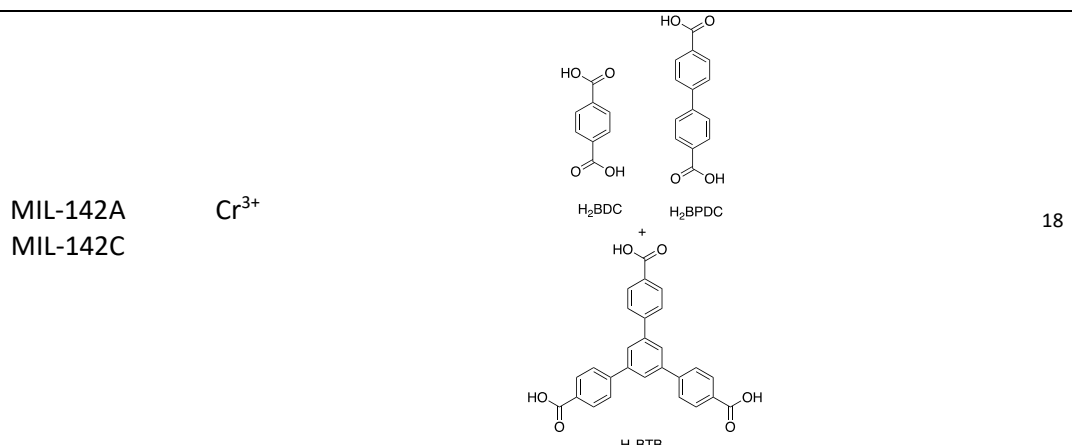
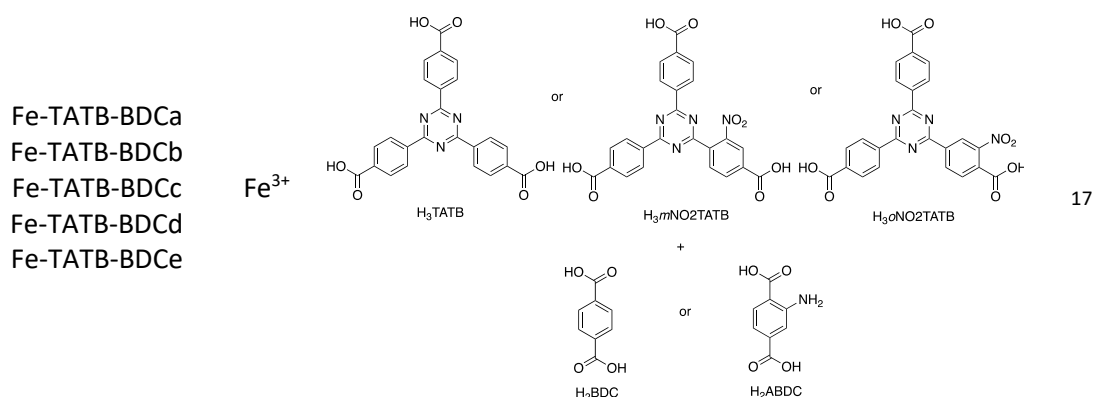
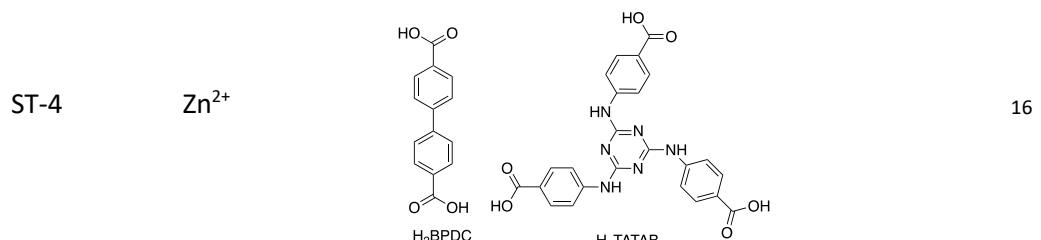
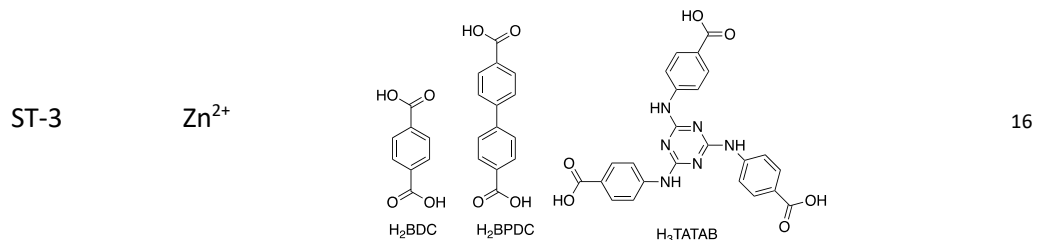


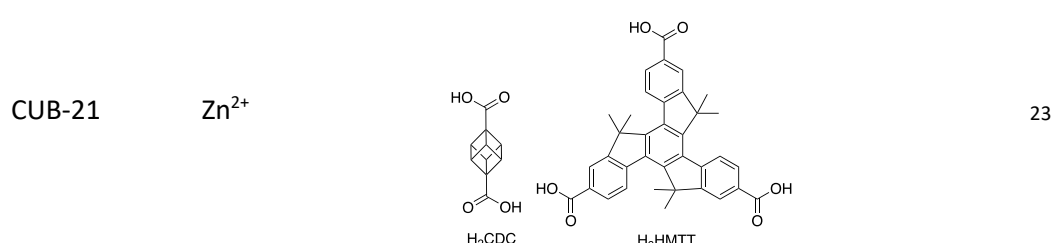
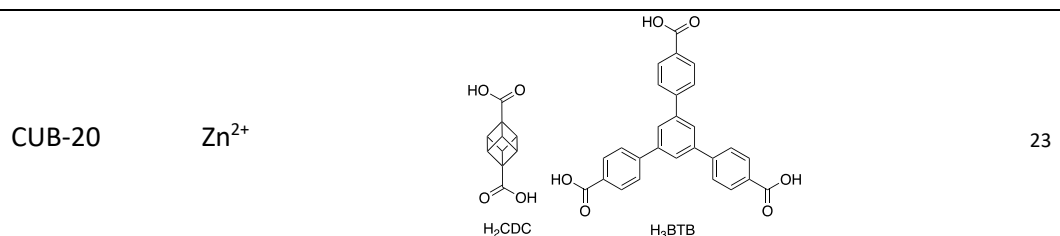
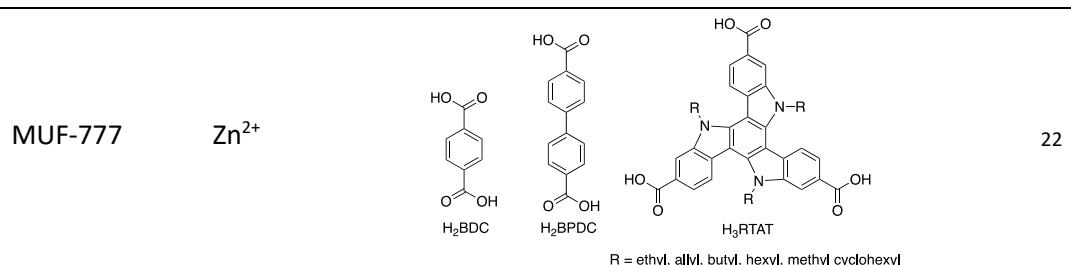
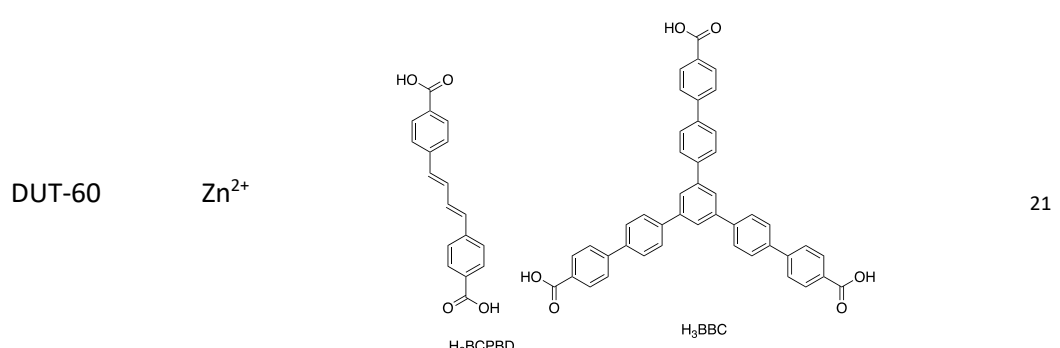
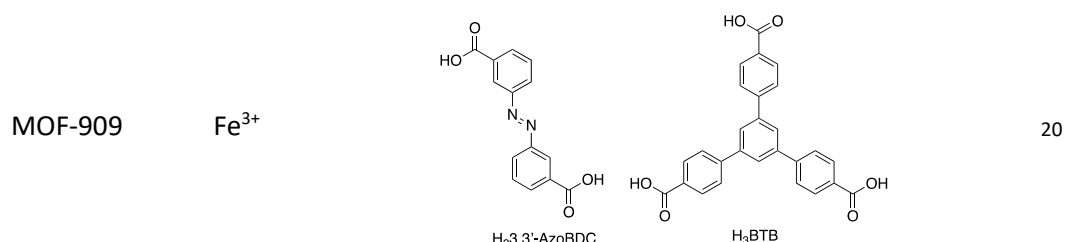
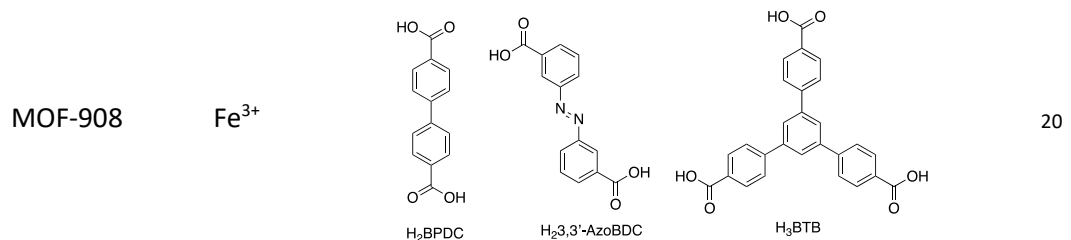
---

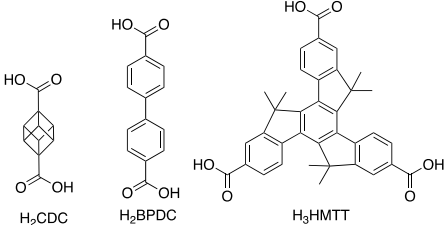
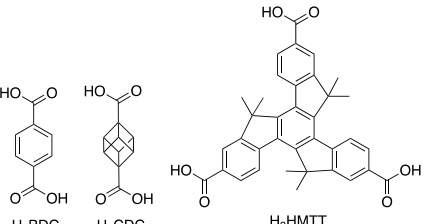
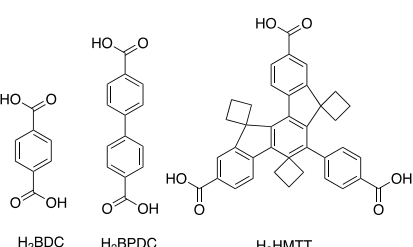
UMCM-11	$Zn^{2+}$	<p>H<sub>2</sub>BDC      H<sub>2</sub>EDDB      H<sub>2</sub>NTB</p>	10
UMCM-12	$Zn^{2+}$	<p>H<sub>2</sub>BDC      H<sub>2</sub>TMTPDC      H<sub>2</sub>NTB</p>	10
DUT-32	$Zn^{2+}$	<p>H<sub>2</sub>BPDC      H<sub>3</sub>BTCTB</p>	11
PCN-280	$Fe^{3+}$	<p>H<sub>2</sub>BPDC      H<sub>3</sub>BTB</p>	12
PCN-285	$Fe^{3+}$	<p>H<sub>2</sub>4,4'-AzoDC      H<sub>3</sub>BTB</p>	12

---







CUB-30	Zn <sup>2+</sup>		23
CUB-31	Zn <sup>2+</sup>		23
MUF-88-cb	Zn <sup>2+</sup>		24

**Table ST7:** Measured and theoretical micropore volumes and BET surface area of MIL-142(Sc) series

MOF	Micropore Volumes (cm <sup>3</sup> g <sup>-1</sup> )		BET Surface Area (m <sup>2</sup> g <sup>-1</sup> )*
	Measured	Theoretical	
MIL-142(Sc)-TATB	0.70	0.70	1768
MIL-142(Sc)-TATB-NH <sub>2</sub>	0.57	0.66	1497
MIL-142(Sc)-TATB-NO <sub>2</sub>	0.56	0.63	1468
MIL-142(Sc)-PTB	0.66	0.70	1688
MIL-142(Sc)-PTB-NH <sub>2</sub>	0.59	-	1508
MIL-142(Sc)-PTB-NO <sub>2</sub>	0.57	-	1415

Note: BET surface areas of MIL-142(Sc) series are included for comparison with reported values of MIL-142(Fe) analogues.

Measured & theoretical micropore volumes for MIL-142(Fe) analogues (measured; theoretical) (cm<sup>3</sup> g<sup>-1</sup>): MIL-142A, 0.70; 0.75; MIL-142ANH<sub>2</sub>, 0.69; 0.70 and MIL-142ANO<sub>2</sub>, 0.68; 0.69.

Measured & theoretical BET surface area for MIL-142(Fe) analogues (measured; theoretical)<sup>8</sup> (m<sup>2</sup> g<sup>-1</sup>): MIL-142A, 1580; 1900; MIL-142ANH<sub>2</sub>, 1390; 1660 and MIL-142ANO<sub>2</sub> 1340; 1600.

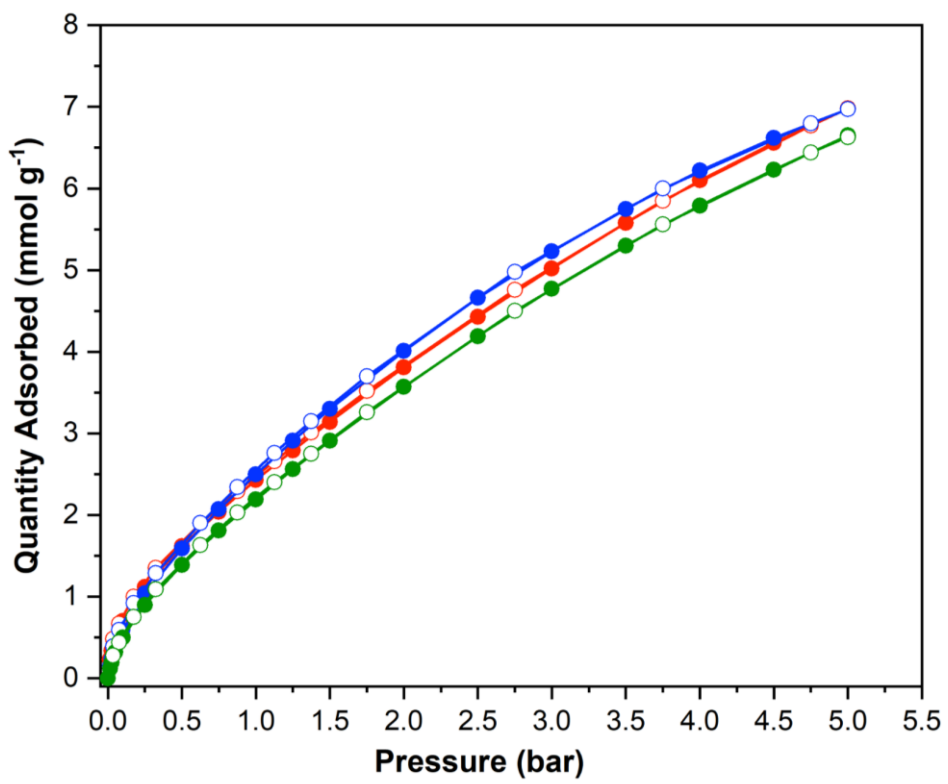


**Figure S21:** CO<sub>2</sub> adsorption isotherms of MIL-142(Sc)-TATB (red), (b) MIL-142(Sc)-TATB-NH<sub>2</sub> (blue) and (c) MIL-142(Sc)-TATB-NO<sub>2</sub> (green).

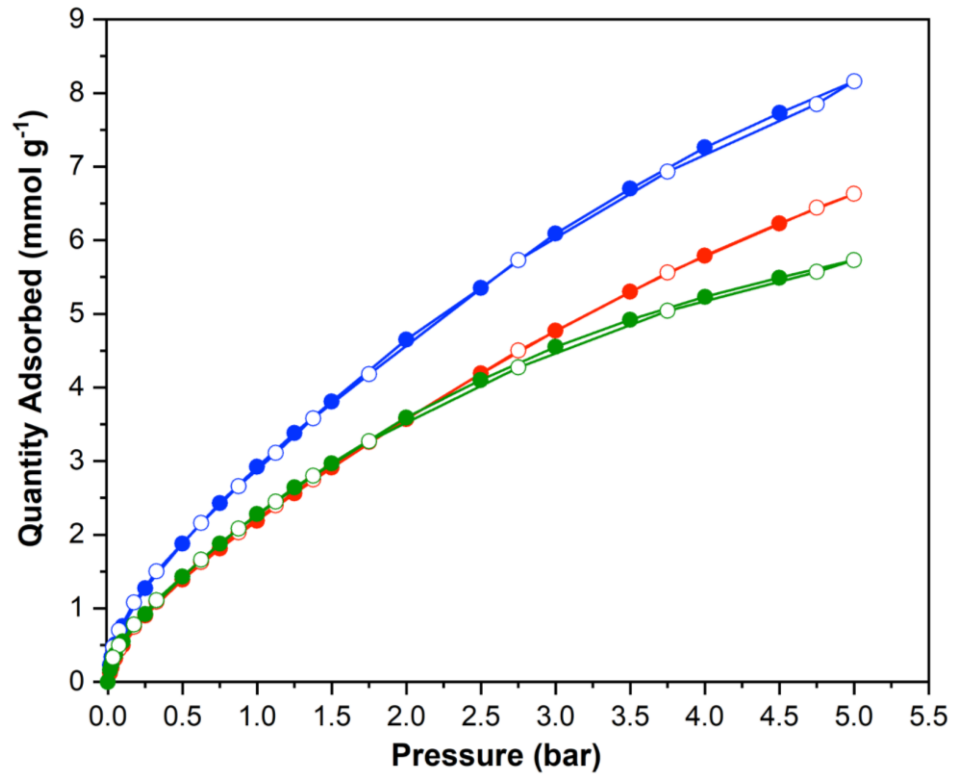
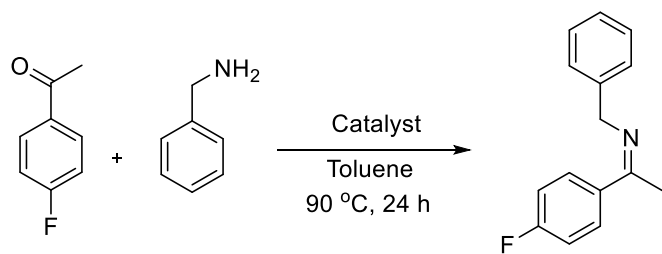


**Figure S22:** CO<sub>2</sub> adsorption isotherms at 298 K of MIL-142(Sc)-PTB (red), (b) MIL-142(Sc)-PTB-NH<sub>2</sub> (blue) and (c) MIL-142(Sc)-PTB-NO<sub>2</sub> (green).



**Scheme SS2:** Imine condensation between 4'-fluoroacetophenone and benzyl amine. Reaction conditions: 1 mmol of 4'-fluoroacetophenone, 1.3 mmol benzyl amine and 1.5 mol % catalyst in 5 mL toluene at 363 K for 24 h. Conversions were determined by <sup>19</sup>F NMR spectroscopy.

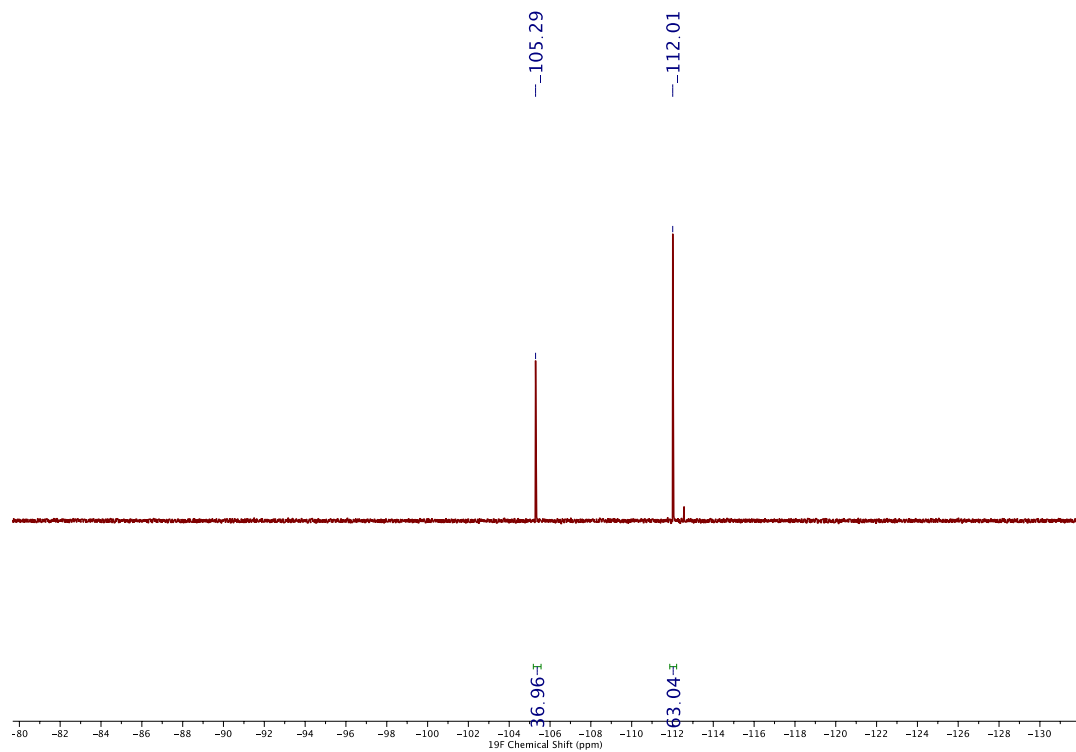


**Figure S23:** <sup>19</sup>F NMR of imine condensation catalysed by MIL-142(Sc)-TATB.

## References

- 1 E. Mühlbauer, A. Klinkebiel, O. Beyer, F. Auras, S. Wuttke, U. Lüning and T. Bein, *Microporous Mesoporous Mater.*, 2015, **216**, 51–55.
- 2 J. Park, D. Feng and H. C. Zhou, *J. Am. Chem. Soc.*, 2015, **137**, 11801–11809.
- 3 K. Koh, A. G. Wong-Foy and A. J. Matzger, *Angew. Chemie - Int. Ed.*, 2008, **47**, 677–680.
- 4 K. Koh, A. G. Wong-Foy and A. J. Matzger, *J. Am. Chem. Soc.*, 2009, **131**, 4184–4185.
- 5 K. Koh, A. G. Wong-Foy and A. J. Matzger, *J. Am. Chem. Soc.*, 2010, **132**, 15005–15010.
- 6 N. Klein, I. Senkovska, K. Gedrich, U. Stoeck, A. Henschel, U. Mueller and S. Kaskel, *Angew. Chemie - Int. Ed.*, 2009, **48**, 9954–9957.
- 7 H. Furukawa, N. Ko, Y. B. Go, N. Aratani, S. B. Choi, E. Choi, A. Ö. Yazaydin, R. Q. Snurr, M. O’Keeffe, J. Kim and O. M. Yaghi, *Science (80-.)*, 2010, **329**, 424–428.
- 8 H. Chevreau, T. Devic, F. Salles, G. Maurin, N. Stock and C. Serre, *Angew. Chemie - Int. Ed.*, 2013, **52**, 5056–5060.
- 9 L. Liu, K. Konstas, M. R. Hill and S. G. Telfer, *J. Am. Chem. Soc.*, 2013, **135**, 17731–17734.
- 10 A. Dutta, A. G. Wong-Foy and A. J. Matzger, *Chem. Sci.*, 2014, **5**, 3729–3734.
- 11 R. Grünker, V. Bon, P. Müller, U. Stoeck, S. Krause, U. Mueller, I. Senkovska and S. Kaskel, *Chem. Commun.*, 2014, **50**, 3450–3452.
- 12 D. Feng, K. Wang, Z. Wei, Y. P. Chen, C. M. Simon, R. K. Arvapally, R. L. Martin, M. Bosch, T. F. Liu, S. Fordham, D. Yuan, M. A. Omari, M. Haranczyk, B. Smit and H. C. Zhou, *Nat. Commun.*, 2014, **5**, 1–9.
- 13 J. Cornelio, T. Y. Zhou, A. Alkaş and S. G. Telfer, *J. Am. Chem. Soc.*, 2018, **140**, 15470–15476.
- 14 S. Yuan, J. S. Qin, L. Zou, Y. P. Chen, X. Wang, Q. Zhang and H. C. Zhou, *J. Am. Chem. Soc.*, 2016, **138**, 6636–6642.
- 15 S. J. Lee, C. Doussot and S. G. Telfer, *Cryst. Growth Des.*, 2017, **17**, 3185–3191.
- 16 C. C. Liang, Z. L. Shi, C. T. He, J. Tan, H. D. Zhou, H. L. Zhou, Y. Lee and Y. B. Zhang, *J. Am. Chem. Soc.*, 2017, **139**, 13300–13303.
- 17 E. Virmani, O. Beyer, U. Lüning, U. Ruschewitz and S. Wuttke, *Mater. Chem. Front.*, 2017, **1**, 1965–1974.
- 18 J. H. Wang, Y. Zhang, M. Li, S. Yan, D. Li and X. M. Zhang, *Angew. Chem. Int. Ed.*, 2017, **56**, 6478–6482.
- 19 H. L. Nguyen, T. T. Vu, D. K. Nguyen, C. A. Trickett, T. L. H. Doan, C. S. Diercks, V. Q. Nguyen and K. E. Cordova, *Commun. Chem.*, 2018, **1**, 1–7.
- 20 T. T. M. Nguyen, H. M. Le, Y. Kawazoe and H. L. Nguyen, *Mater. Chem. Front.*, 2018, **2**, 2063–2069.
- 21 I. M. Hönicke, I. Senkovska, V. Bon, I. A. Baburin, N. Bönisch, S. Raschke, J. D. Evans and S. Kaskel, *Angew. Chem. Int. Ed.*, 2018, **57**, 13780–13783.
- 22 A. Alkaş, J. Cornelio and S. G. Telfer, *Chem. - An Asian J.*, 2019, **14**, 1167–1174.
- 23 L. K. Macreadie, R. Babarao, C. J. Setter, S. J. Lee, O. T. Qazvini, A. J. Seeber, J. Tsanaktsidis, S. G. Telfer, S. R. Batten and M. R. Hill, *Angew. Chem. Int. Ed.*, 2020, **59**, 6090–6098.
- 24 A. Alkaş, L. E. S. Friche, S. N. Harris and S. G. Telfer, *Chem. - A Eur. J.*, 2020, **26**, 10321–10329.